

ON THE RADIAL DYNAMICS OF FRICTION DISCS

Alexander Fidlin

LuK GmbH & Co. oHG, Bühl
Germany
alexander.fidlin@schaeffler.com

Wolfgang Stamm

LuK GmbH & Co. oHG, Bühl
Germany
stammwol@schaeffler.com

Abstract

An analytical and numerical study of the radial dynamics of friction discs is presented. Of particular interest are two types of motion which are characteristic for the considered systems: self centering of the friction disc at the low rotation speeds and the seeming “instability” of this equilibrium at high speeds. It is shown that the last one leads to a limit cycle with large radial displacements and intensive slip between the discs. The amplitude of the limit cycle is limited by damping in the simplest case of linear springs. In reality the amplitude can be limited by different kinds of nonlinearity both in radial or in normal directions. These two types of motion exist alongside with pure sticking already in the simplest pin-on-the-disc apparatus which is a standard experimental setup for investigations of the friction coefficient. The strong coupling between the torsion and radial modes appears as an additional effect in a system of two rotating discs with the frictionally transmitted torque. It is shown that this coupling can destabilize the limit cycle and create a new one with slowly modulated amplitude. All analytical results are compared with numerical simulations.

Key words

Friction, pin on rotating disc, disc on rotating disc, instability, critical rotation speed

1 Introduction

Rotating friction discs are usual in various technical applications. Dry and wet friction clutches in automotive transmissions [Reik, 1994] can be mentioned here alongside with clutch actuation bearings [Zink, 2002]. Great attention was paid in the past to various dynamic phenomena in the slider – disc contact [Honchi, 2003; Ibrahim, 1994a; Ibrahim, 1994b; Tworzydło, 1994]. The main applications here are the standard test rigs for measurement of the friction coefficient [Ibrahim, 1994a], friction brakes [Wallaschek, 1999] and magnetic disc drives [Honchi, 2003]. However, the majority of the publications is concentrated either on the investigations of the friction coefficient itself or on the

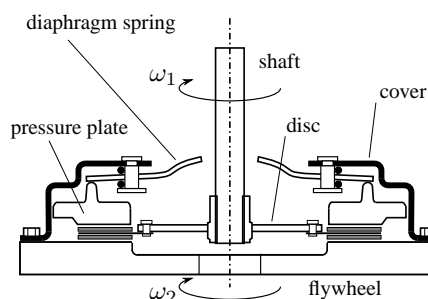


Figure 1. Standard dry friction clutch

coupling of tangential and normal modes with respect to the disc’s surface [Mottershead, 2001]. It is usually suggested that the pin’s support is much stiffer than the critical value determined by the considered range of the disc’s rotation speeds.

In several technical applications, especially in dry friction clutches and clutch actuation systems, the situation is significantly different. Clutches usually operate in a speed range between 0 and 6000 rpm and under certain conditions the corresponding frequency might be higher than the natural frequency of the friction disc mounted on the input shaft of the transmission (cf. Fig. 1). This fact combined with usual manufacturing tolerances (especially the eccentricity of the input shaft with respect to the flywheel) can cause various undesired effects like chatter [Albers, 1998] or extremely high wear at the friction surfaces. The last problem became even more important in combination with slip control [Kuepper, 2002; Kuepper, 2006] which can be used in order to reduce torsion vibrations in automotive transmissions.

In the present paper we firstly investigate the radial dynamics of the classical pin-on-the-disc system both for sub- and supercritical rotation speeds. Then the obtained results are generalized for the disc-on-the-disc system. An additional effect of the coupling between the torsion and radial dynamics leading to interesting instability phenomena occurs here. Due to the practical importance of systems with permanently

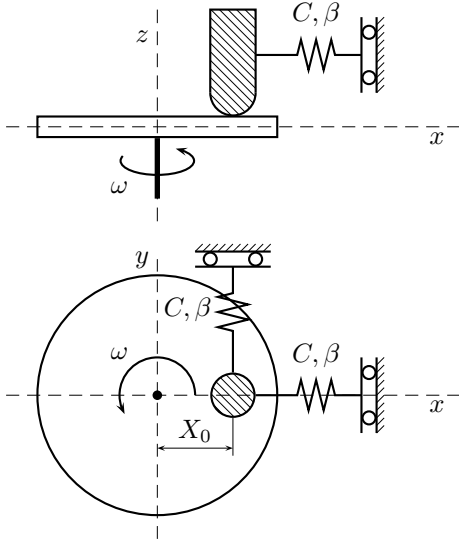


Figure 2. Pin on the rotating disc

controlled slip, the analysis is mainly restricted to the pure slip motions. The not least important phenomena with alternating stick and slip phases which can occur here even for constant friction coefficient will be discussed separately on the basis of the regularized two-dimensional friction contact model [Stamm, 2006].

2 Radial Dynamics of a Pin on Rotating Disc at Low Rotating Speeds

Consider the classical pin-on-the-disc shown in Fig. 2. The system consists of a pin (mass m) which can move on the surface of the disc rotating at a constant angular speed ω . The pin is supported in both x and y directions by springs characterized by their stiffness C and damping coefficient β . Point $(X_0, 0)$ corresponds to the relaxed state of the springs. The coupling between the pin and the disc is described by Coulomb's friction law with the friction coefficient μ and the normal load N .

Equations of motion of the pin are as follows:

$$\begin{aligned} m\ddot{x} + \beta\dot{x} + C(x - X_0) &= \frac{-\mu N(\dot{x} + \omega y)}{\sqrt{(\dot{x} + \omega y)^2 + (\dot{y} - \omega x)^2}} \\ m\ddot{y} + \beta\dot{y} + Cy &= \frac{-\mu N(\dot{y} - \omega x)}{\sqrt{(\dot{x} + \omega y)^2 + (\dot{y} - \omega x)^2}} \end{aligned} \quad (1)$$

Converting to the polar coordinates,

$$x = \rho \cos \psi; \quad y = \rho \sin \psi \quad (2)$$

it is easy to calculate the stationary solutions of (1) corresponding to the equilibrium of the pin in space and

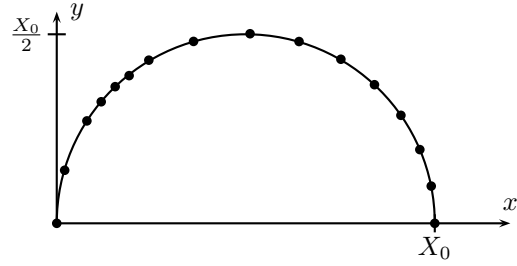


Figure 3. Equilibriums of the sliding pin for different values of the normal load

permanent slip between the pin and the disc:

$$\begin{aligned} \rho_* &= \sqrt{X_0^2 - \frac{\mu^2 N^2}{C^2}}; \quad \psi_* = \arcsin \frac{\mu N}{CX_0} \\ x_* &= X_0 \left(1 - \frac{\mu^2 N^2}{C^2 X_0^2}\right); \quad y_* = \frac{\mu N}{CX_0} \sqrt{X_0^2 - \frac{\mu^2 N^2}{C^2}} \end{aligned} \quad (3)$$

One can notice that this solution always satisfies the following equation:

$$\left(x_* - \frac{X_0}{2}\right)^2 + y_*^2 = \frac{X_0^2}{4} \quad (4)$$

This equation describes the circle going through the rotation axis and the relaxed point of the springs. Fig. 3 shows the comparison of the analytic prediction (3) (solid line) and numeric simulations of the equations (1) (dots).

If one increases the load N , the equilibrium moves along the semicircle towards the rotation axis. It is important to notice that the equilibrium exists as long as the normal load is sufficiently small:

$$\mu N \leq CX_0 \quad (5)$$

This effect is often interpreted as the so called self centering of the elastically supported mass on the rotating disc. One can show that this equilibrium remains always stable in its existence domain (5).

If the normal load is sufficiently large, sticking becomes possible, i.e. the pin finds its equilibrium on the disc and rotates with the disc in the inertial space. This type of solutions satisfies the following equations:

$$\begin{aligned} m\ddot{x} + \beta\dot{x} + C(x - X_0) &= F_{Rx} \\ m\ddot{y} + \beta\dot{y} + Cy &= F_{Ry} \\ F_R &= \sqrt{F_{Rx}^2 + F_{Ry}^2} \leq \mu N \end{aligned} \quad (6)$$

Supposing $x = A \cos \omega t$; $y = A \sin \omega t$, one obtains the following condition for the existence of the sticking

equilibrium:

$$\mu^2 N^2 \geq (C - m\omega^2)^2 A^2 + \beta^2 A^2 \omega^2 + C^2 X_0^2 - 2CX_0A [(C - m\omega^2) \cos \omega t - \beta \omega \sin \omega t] \quad (7)$$

This inequality must be fulfilled for any t . It is the case as soon as the following inequality holds:

$$\sqrt{(C - m\omega^2)^2 + \beta^2 \omega^2} A + CX_0 \leq \mu N \quad (8)$$

This inequality can be interpreted in two different ways. Firstly, it means, as soon as the normal load becomes larger than the threshold (5), sticking solution is possible. Secondly, the domain of the possible sticking on the disc is limited due to the following inequality for the amplitude A , which is the distance between the pin and the rotation axis:

$$A \leq \frac{\mu N - CX_0}{\sqrt{(C - m\omega^2)^2 + \beta^2 \omega^2}}, \quad \mu N > CX_0 \quad (9)$$

Note that the right hand side of the first inequality has a typical resonant structure, which means that the sticking domain firstly increases with the increasing rotation speed, then it reaches its maximum at

$$\omega_* = \sqrt{\frac{C}{m} - \frac{\beta^2}{2m^2}}$$

(if β sufficiently small) and then decreases. The sticking domain becomes arbitrarily small for sufficiently large rotation speeds ω .

3 Radial Dynamics of a Pin on Rotating Disc at High Rotating Speeds

Another type of periodic solution becomes important at high rotation speeds. In order to obtain this solution let us convert (1) to the polar coordinates (2):

$$\begin{aligned} m\ddot{\rho} - m\rho\dot{\psi}^2 + \beta\dot{\rho} + C\rho - CX_0 \cos \psi &= \frac{-\mu N \dot{\rho}}{\sqrt{\dot{\rho}^2 + \rho^2(\omega - \dot{\psi})^2}} \\ m\rho\ddot{\psi} + 2m\dot{\rho}\dot{\psi} + \beta\rho\dot{\psi} + CX_0 \sin \psi &= \frac{\mu N \rho(\omega - \dot{\psi})}{\sqrt{\dot{\rho}^2 + \rho^2(\omega - \dot{\psi})^2}} \end{aligned} \quad (10)$$

Firstly, we consider the simplified case $X_0 = 0$, which means, there is no static eccentricity between the disc and the pin. Then the following solution always exists:

$$\dot{\psi} = k = \sqrt{\frac{C}{m}}; \quad \rho = \rho_c = \frac{\mu N}{\beta k}; \quad \dot{\rho} = 0 \quad (11)$$

It is interesting to notice that the amplitude of the pin in this solution is limited only by the damping in the linear springs. In practical application the amplitude is usually limited by nonlinearities either of the radial or of the normal forces which then both depend on the radial displacement of the pin.

Let us now investigate the stability of the considered solution. Introducing variations and linearizing (10) in the vicinity of the equilibrium (11) we obtain the following equations:

$$\begin{aligned} \dot{\psi} &= k + \eta; \quad \rho = \rho_c + \xi; \quad \dot{\rho} = \dot{\xi} \\ \ddot{\xi} + \frac{\beta}{m} \frac{\omega}{\omega - k} \dot{\xi} - \frac{2\mu N}{\beta} \eta &= 0 \\ \dot{\eta} + \frac{\beta}{m} \eta + \frac{\beta k^2}{\mu N} \left(2\dot{\xi} + \frac{\beta}{m} \xi \right) &= 0 \end{aligned} \quad (12)$$

The characteristic equation is as follows:

$$\lambda^3 + \left(1 + \frac{\beta}{m} \frac{\omega}{\omega - k} \right) \lambda^2 + \left(\frac{\beta^2}{m^2} \frac{\omega}{\omega - k} + 4k^2 \right) \lambda + 2k^2 \frac{\beta}{m} = 0 \quad (13)$$

All the solutions of this equation have negative real parts if according to Hurwitz' criterion the following inequalities are fulfilled:

$$\frac{\omega}{\omega - k} > -1; \quad \frac{\omega}{\omega - k} > -\frac{4k^2 m^2}{\beta^2} \quad (14)$$

and

$$\frac{\omega}{\omega - k} < -\frac{1}{2} \left[1 + \frac{4k^2 m^2}{\beta^2} + \sqrt{1 + \left(\frac{4k^2 m^2}{\beta^2} \right)^2} \right] \quad (15)$$

or

$$\frac{\omega}{\omega - k} > -\frac{1}{2} \left[1 + \frac{4k^2 m^2}{\beta^2} - \sqrt{1 + \left(\frac{4k^2 m^2}{\beta^2} \right)^2} \right] \quad (16)$$

Inequalities (14) and (15) are incompatible. Inequality (16) is always stronger than (14). Thus, (16) is the necessary and sufficient condition for linear stability of the considered limit cycle. Note that this inequality is automatically fulfilled as soon as the rotation speed ω is larger than the natural frequency of the pin mass attached to one of the springs.

If the eccentricity is small but different from zero, i.e. $X_0 \neq 0$, then the solution can be approximately found as a circle which center is shifted from the rotation axis:

$$x = x_s + A \cos kt; \quad y = y_s + A \sin kt \quad (17)$$

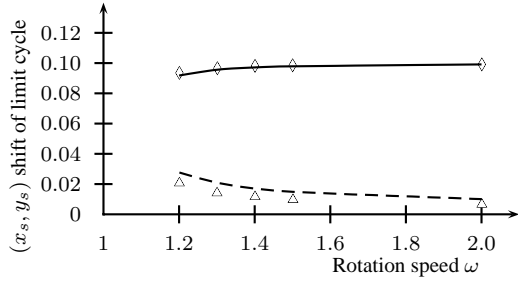


Figure 4. Comparison of the analytic (x_s – solid line; y_s – dashed line) and numeric predictions (x_s – diamonds; y_s – triangles) for the following parameter values: $\mu N = 0.12$; $X_0 = 0.1$; $m = 1$; $C = 1$; $\beta = 0.1$

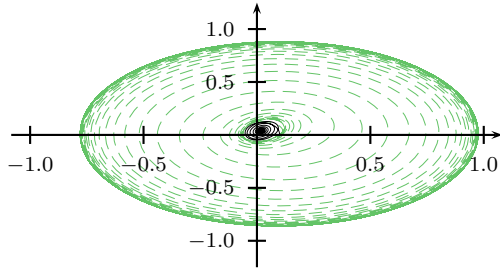


Figure 5. Two different solutions (equilibrium – solid black line, limit cycle – dashed green line) for the following parameter values: $m = 1$; $C = 1$; $\beta = 0.1$; $\mu N = 0.09$; $\omega = 1.5$; $X_0 = 0.1$ and the following initial conditions: $x(0) = 0.1$; $y(0) = \dot{x}(0) = \dot{y}(0) = 0$ for the equilibrium and $x(0) = 0.1$; $\dot{x}(0) = 0.03$; $y(0) = \dot{y}(0) = 0$ for the limit cycle.

Substituting (17) into (1) and balancing the first harmonic terms one obtains the following expressions for the shift of the limit cycle:

$$x_s = \frac{X_0}{1 + \frac{\beta^2 \omega^2}{4mC(\omega-k)^2}}; \quad y_s = \frac{\beta \omega x_s}{2mk(\omega-k)} \quad (18)$$

Figure 4 shows a comparison of the approximate prediction (18) with the results of direct numerical simulations.

Figure 5 shows that both equilibrium (3) and limit cycle (17) can coexist for the same parameter values but slightly different initial conditions, i.e. both have limited attraction areas in the phase space.

Finally, Figure 6 shows the typical evolution of the steady state solutions under increasing normal load. It can be noticed that the solution with sticking and the limit cycle with large amplitudes and pure slip exist for the same parameter values.

4 Radial Dynamics of a Rotating Friction Disc

Let us now go further to an investigation of the radial dynamics of a friction disc lying on a rotating disc (cf. Fig. 7). The system consists of a friction disc (mass m , polar inertia J) which can move on the surface of the master disc rotating at a constant angular speed ω .

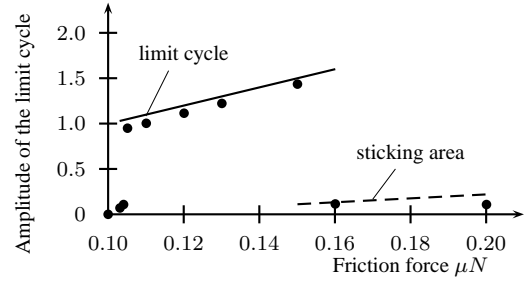


Figure 6. Evolution of the steady state solutions for the same parameter values as in Fig. 4, but $\omega = 1.2$

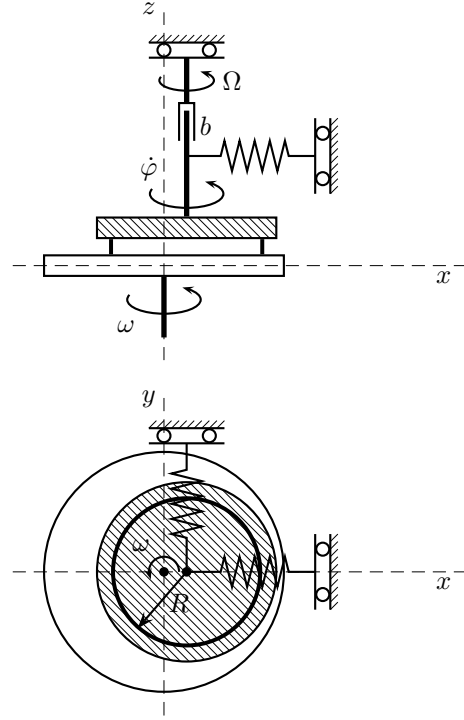


Figure 7. Friction disc on the rotating master disc

The friction disc is supported in both x and y directions by springs characterized by their stiffness C and damping coefficient β . Point $(X_0, 0)$ corresponds to the relaxed state of the springs. The coupling between the two discs along a circle with the radius R is described by the Coulomb's frictions law with the friction coefficient μ and the normal load N .

The disc (with respect only to its torsional degree of freedom) is connected by a viscous element with the damping coefficient b to an infinite mass rotating at a constant velocity Ω . Equations of motion for the friction disc are as follows:

$$\begin{aligned} m\ddot{x} + \beta\dot{x} + C(x - X_0) &= F_x \\ m\ddot{y} + \beta\dot{y} + Cy &= F_y \\ J\ddot{\phi} + b(\dot{\phi} - \Omega) &= M \end{aligned} \quad (19)$$

with

$$\begin{aligned} F_x &= -\frac{\mu N}{2\pi} \int_0^{2\pi} \frac{\nu_{rx}(\chi)}{|\nu_r|} d\chi \\ F_y &= -\frac{\mu N}{2\pi} \int_0^{2\pi} \frac{\nu_{ry}(\chi)}{|\nu_r|} d\chi \\ M &= \frac{\mu N}{2\pi} R \int_0^{2\pi} \frac{\tilde{\nu}_r(\chi)}{|\nu_r|} d\chi \end{aligned} \quad (20)$$

Here we use the following symbols (χ is the angle along the contact circle):

$$\begin{aligned} \nu_{rx} &= \dot{x} + \omega y + R(\omega - \dot{\varphi}) \sin(\varphi + \chi) \\ \nu_{ry} &= \dot{y} - \omega x - R(\omega - \dot{\varphi}) \cos(\varphi + \chi) \\ |\nu_r| &= \sqrt{\nu_{rx}^2 + \nu_{ry}^2} \\ \tilde{\nu}_r &= \nu_{rx} \sin(\varphi + \chi) - \nu_{ry} \cos(\varphi + \chi) \end{aligned} \quad (21)$$

These equations were implemented numerically in the software package ITI-SIM, where the contact ring was discretized in six contact points. In order to avoid unnecessary complications in the qualitative analysis, equations (19), (20) and (21) can be significantly simplified if we replace the modulus of the relative velocity of the contact points through the corresponding Taylor's expansion and take three first terms into account:

$$\begin{aligned} \frac{\tilde{\nu}_r}{|\nu_r|} &= 1 - \frac{R(\omega - \dot{\varphi})}{\bar{\nu}_r^2} \tilde{\nu}_{xy} \\ \bar{\nu}_r &= \sqrt{(\dot{x} + \omega y)^2 + (\dot{y} - \omega x)^2 + R^2(\omega - \dot{\varphi})^2} \\ \tilde{\nu}_{xy} &= (\dot{x} + \omega y) \sin(\varphi + \chi) - (\dot{y} - \omega x) \cos(\varphi + \chi) \end{aligned} \quad (22)$$

Then equations (19) take the following form:

$$\begin{aligned} F_x &= -\frac{\mu N}{\bar{\nu}_r} (\dot{x} + \omega y) \left(1 - \frac{R^2(\omega - \dot{\varphi})^2}{2\bar{\nu}_r^2} + \frac{3}{4}\Phi \right) \\ F_y &= -\frac{\mu N}{\bar{\nu}_r} (\dot{y} - \omega x) \left(1 - \frac{R^2(\omega - \dot{\varphi})^2}{2\bar{\nu}_r^2} + \frac{3}{4}\Phi \right) \\ M &= \frac{\mu N}{\bar{\nu}_r} R^2(\omega - \dot{\varphi}) \left(1 - \frac{\bar{\nu}_{xy}^2}{2\bar{\nu}_r^2} + \frac{3}{4}\Phi \right) \\ \bar{\nu}_{xy}^2 &= (\dot{x} + \omega y)^2 + (\dot{y} - \omega x)^2 \\ \Phi &= \frac{R^2(\omega - \dot{\varphi})^2}{\bar{\nu}_r^2} \cdot \frac{\bar{\nu}_{xy}^2}{\bar{\nu}_r^2} \end{aligned} \quad (23)$$

Let us investigate the steady state solutions of these equations corresponding the equilibrium of the center of the friction disc and its constant rotation speed: $\dot{x} = 0$; $\dot{y} = 0$; $\dot{\varphi} = \text{const}$.

It turns out that these solutions are still located on the semi-circle (4). The simplest way to calculate the equi-

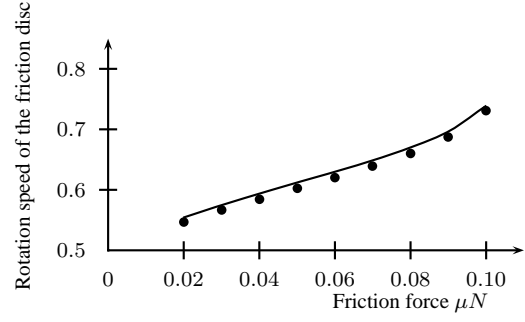


Figure 8. Angular velocity of the friction disc, analytic approximation – solid line, numeric prediction – dots

libriums is to convert to spherical coordinates as follows:

$$\begin{aligned} x &= A \cos \alpha \cos \theta; \quad y = A \cos \alpha \sin \theta \\ \dot{\varphi} &= \omega \left(1 - \frac{A}{R} \sin \alpha \right) \end{aligned} \quad (24)$$

Using the signs

$$\mu_0 = \frac{\mu N}{C}; \quad b_0 = \frac{b\omega}{RC}; \quad \delta = 1 - \frac{\Omega}{\omega} \quad (25)$$

one obtains a trigonometric equation determining the solution:

$$\begin{aligned} \delta &= \frac{\sin \alpha}{R} A + \frac{\mu_0}{b_0} \sin \alpha \left[1 - \frac{1}{2} \cos^2 \alpha \left(1 - \frac{3}{2} \sin^2 \alpha \right) \right] \\ A &= \sqrt{\frac{X_0^2}{\cos^2 \alpha} - \mu_0^2 \left(1 - \frac{1}{2} \cos^2 \alpha + \frac{3}{16} \sin^2 \alpha \right)^2} \\ \theta &= \arccos \left(\frac{A}{X_0} \cos \alpha \right) \end{aligned} \quad (26)$$

Figure 8 shows comparisons of the analytic approximation for the angular velocity of the friction disc (24), (26) with the numeric solutions of the system (19), (20) and (21). The simulations were performed for the following parameter values: $m = 1$; $J = 1$; $C = 1$; $R = 0.12$; $b = 0.01$; $\omega = 0.8$; $\Omega = 0.5$; $\beta = 0.003$

Solutions with large amplitudes and permanent slip also exist here alongside with sticking. Figures 9 and 10 show a comparison of the analytic and numeric predictions for the same parameter values as above, but $\omega = 1.5$; $\Omega = 1.25$.

However the most interesting difference between the pin-on-the-disc and disc-on-the-disc is the possibility of strong interaction between the torsion dynamics of the disc and its radial motions. An impressive illustration of this interaction can be seen in Fig. 11 which demonstrates a typical solution in case of the instability of the limit cycle with large amplitudes at high rotation speeds for the following parameter values: $m = 1$; $J = 1$; $C = 1$; $R = 0.12$; $b = 0.015$; $\omega = 1.5$; $\Omega = 1.25$; $\beta = 0.5$; $\mu N = 0.0225$

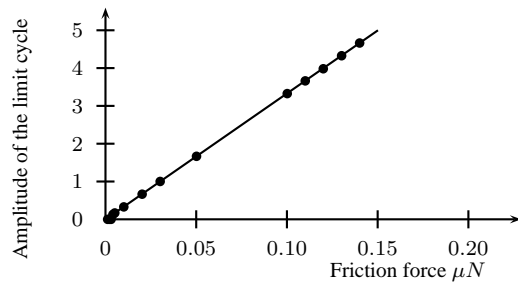


Figure 9. Comparison of the steady state solutions for the friction disc at large rotation speed of the master disc, analytic approximation – solid line, numeric prediction – dots

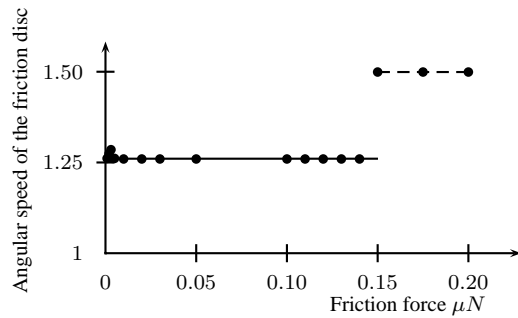


Figure 10. Comparison of the stationary rotation speed, analytic approximation (large limit cycle with permanent slip) – solid line, numeric prediction – dots, sticking – dashed line

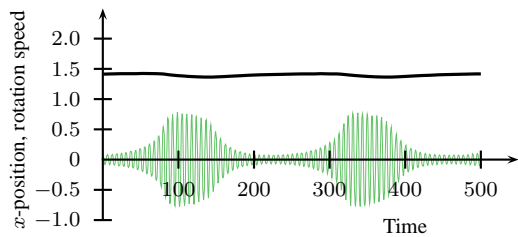


Figure 11. Complex limit cycle of the friction disc with slowly modulated amplitudes of its rotation speed (heavy black line) and radial position (light green line shows the x -position of the disc's center multiplied by 20)

Note that the existence region of this complex limit cycle can be investigated analytically by a stability analysis for the basic limit cycle with large amplitudes similar to that performed on the pin on the disc, however it would blow up the limits of this article.

5 Conclusions

Radial dynamics of a friction disc is in many aspects similar to that of a pin on a rotating disc. Self-centering is typical for both systems at low rotation speeds. At high rotation speeds the equilibrium corresponding to the self-centering still remains stable but its attraction area shrinks. Outside this attraction area solutions tend to a limit cycle with large radial displacements and intensive slip between the disks. The amplitude of the limit cycle is limited by damping in the simplest case

of linear springs. In reality, the amplitude can be limited by different kinds of nonlinearity both in radial or normal directions. These two types of motion exist alongside with pure sticking already in the simplest pin-on-the-disc system. The strong coupling between the torsion and radial modes appears as an additional effect in a system of two rotating discs with the frictionally transmitted torque. It is shown that this coupling can destabilize the limit cycle and create a new one with slowly modulated amplitude.

References

- Albers A. and Herbst D. (1998) Chatter – causes and solutions. *6th LuK Symposium*, pp. 23–45
- Honchi M., Kohira H. and Matsumoto M. (2003) Numerical simulation of slider dynamics during slider – disk contact. *Tribology International* 36, pp. 235–240
- Ibrahim R. A. (1994) Friction-induced vibration, chatter, squeal and chaos: Part I – Mechanics of contact and friction. *Applied Mechanics Reviews* 47, pp. 209–226
- Ibrahim R. A. (1994) Friction-induced vibration, chatter, squeal and chaos: Part II – Dynamics and Modeling. *Applied Mechanics Reviews* 47, pp. 227–254
- Kuepper K., Seebacher R. and Werner O. (2002) Think systems – software by LuK. *7th LuK Symposium*, pp. 219–230
- Kuepper K., Serebrennikov B. and Goepfert G. (2006) Software for automatized transmissions – intelligent driving. *8th LuK Symposium*, pp. 155–168
- Mottershead J. E. (2001) Vibrations and friction-induced instability in discs. In Guran A., Pfeiffer F. and Popp K. (Eds.) *Dynamics with Friction: Modeling, Analysis and Experiment, Part II*. World Scientific, pp. 29–74
- Reik W. (1994) The Self-Adjusting Clutch. *5th LuK Symposium*, pp. 43–63
- Stamm W. and Fidlin A. (2006) Regularization of 2D frictional contacts for rigid body dynamics. In Eberhard P. (Ed.) *IUTAM Symposium on Multiscale Problems in Multibody System Contacts*. Springer, pp. 291–300
- Tworzydło W. W., Becker E. B. and Oden J. T. (1994) Numerical modeling of friction-induced vibrations and dynamic instabilities. *Applied Mechanics Reviews* 47, pp. 255–274
- Wallaschek J., Hach K., Stolz U. and Mody P. (1999) A survey of the present state of friction modeling in the analytical and numerical investigation of brake noise generation. *Proceedings of the ASME Vibration Conference*, ASME Design Engineering Technical Conferences, Las Vegas, pp. 12–15
- Zink M., Sheard R. and Welter R. (2002) Clutch release systems. *7th LuK Symposium*, pp. 35–47